

AN OPTION OF HIGH CHARGE OPERATION FOR THE EUROPEAN XFEL

M. Krasilnikov^{*}, G. Asova[†], H.J. Grabosch, M. Groß, L. Hakobyan, I.V. Isaev[‡],
Y. Ivanisenko, M. Khojoyan[§], G. Klemz, M. Mahgoub, D.A. Maljutin, A. Oppelt,
M. Otevre, B. Petrosyan, S. Rimjaem, A. Shapovalov[‡], F. Stephan,
G. Vashchenko, S. Weidinger, DESY, 15738 Zeuthen, Germany
E.A. Schneidmiller, M.V. Yurkov, DESY, 22607 Hamburg, Germany
I. Templin, I. Will, MBI, 12489 Berlin, Germany
D. Richter, HZB, 14109 Berlin, Germany

Abstract

The 1.3 GHz superconducting accelerator developed in the framework of TESLA and the European XFEL project holds the potential to accelerate high charge electron beams. This feature has been successfully demonstrated during the first run of the free electron laser at the TESLA Test Facility with lasing driven by electron bunches with a charge of up to 4 nC. Currently DESY and the European XFEL GmbH perform revision of the baseline parameters for the electron beam. In this report we discuss a potential option of operation of the European XFEL driven by high charge (1 nC to 3 nC) electron beams. We present the results of the production and characterization of high charge electron bunches. Experiments have been performed at PITZ and demonstrated good properties of the electron beam in terms of emittance. Simulations of the radiation properties of SASE FELs show that application of high charge electron beams will open up the possibility to generate radiation pulse energies up to the few hundred milli-Joule level.

INTRODUCTION

Baseline parameters of the European XFEL [1] have been updated recently based on the analysis of recent experimental results obtained at FLASH, LCLS, PITZ, and the results of s2e simulations [2-8]. The range of the charges is between 20 pC and 1 nC. However, it has been discussed earlier that accelerators based on TESLA technology hold the great potential to operate with higher charges. The benefit of operation of the FEL with higher charges may be higher radiation pulse energy (higher number of photon per pulse). For instance, the first free electron laser at FLASH (known as TTF FEL - TESLA Test Facility FEL) operated with bunch charges up to 4 nC [9].

The Photo Injector Test facility at DESY in Zeuthen (PITZ) develops electron sources for linac based short wavelength FELs like FLASH and the European XFEL. The PITZ research program focuses on the beam

emittance minimization at various bunch charge levels by means of extensive photo injector optimization [10].

HIGH CHARGE BUNCHES AT PITZ

The electron source at PITZ is a 1.6-cell normal conducting L-band cavity with a Cs₂Te photo cathode at the backplane. The gun cavity is surrounded by main and bucking solenoids which form a magnetic lens to counteract the beam quality degradation from the space charge forces. Another manner to optimize the phase space of the electron beam is the temporal shaping of the cathode laser. The photo cathode laser system at PITZ was developed by the MBI, Berlin and is capable to produce laser pulses with a flat-top temporal profile of ~20...22 ps FWHM and rise/fall times of ~2 ps [11]. Transverse laser shaping is realized by imaging of a so-called beam shaping aperture (BSA) with variable diameter onto the cathode. A typical laser temporal profile and transverse distribution are shown in Fig. 1.

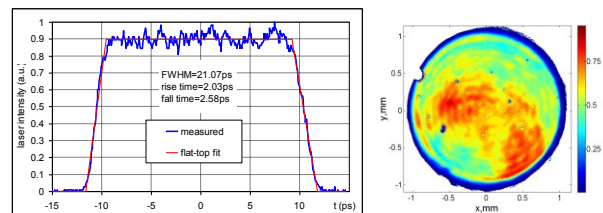


Figure 1: Cathode laser temporal profile measured using an optical sampling system (left). The FWHM of the pulse is 21.1 ps, rise/fall time is 2.0/2.6 ps. Transverse distribution of the photocathode laser pulse (right). The BSA diameter is 2.0 mm, x/y rms sizes are 0.50/0.49 mm.

The PITZ RF-gun accelerates electron beams up to a mean momentum of ~6.7 MeV/c, for further acceleration a CDS booster cavity [10] is used. Currently the maximum beam mean momentum at PITZ is ~25 MeV/c.

Emittance Measurements for 2nC

In order to minimize the projected emittance at PITZ several machine parameters have to be tuned – most important main solenoid current, laser transverse size at the cathode, RF gun launch phase. The booster cavity is usually operated on-crest at the maximum available gradient.

* mikhail.krasilnikov@desy.de

† On leave from INRNE, Sofia, Bulgaria

‡ On leave from MEPHL, Moscow, Russia

§ On leave from YerPhI, Yerevan, Armenia

The projected transverse emittance of an electron beam at PITZ is measured using a slit mask technique. The local beam divergence is measured using a 1 mm thick Tungsten slit with 10 μm opening. The space charge dominated beam is cut into emittance dominated beamlets which are to be measured 2.64 m downstream of the slit mask location. To obtain more details of the transverse phase space a single slit scan is being used, where beamlets are recorded continuously while a slit mask is slowly being moved across the electron beam (with a typical speed of $\sim 0.1 \dots 0.5$ mm/s). With an electron bunch train repetition rate at PITZ of 10 Hz typically up to several hundreds of beamlets are used in the phase space reconstruction.

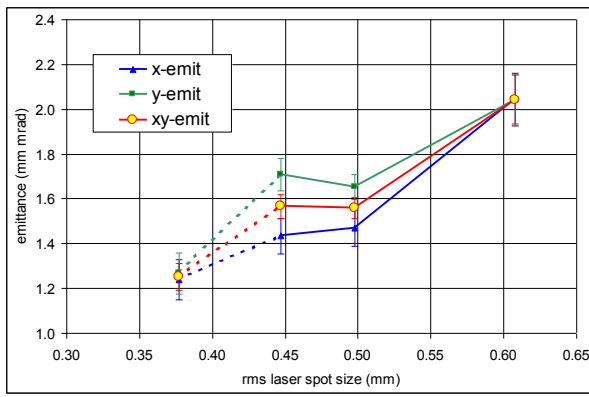


Figure 2: Measured normalized projected emittance as a function of the rms laser spot size at the cathode for a bunch charge of 2 nC. The geometric mean xy-emittance is defined as $\varepsilon_{xy} = \sqrt{\varepsilon_x \varepsilon_y}$.

The PITZ photo injector has been optimized at various levels of the bunch charge [10] – from 20 pC to 2 nC. For this paper the 2 nC case is of most importance. Several laser spot sizes have been tested to minimize the beam emittance. Applied BSA diameters of 1.5, 1.8, 2.0 and 2.5 mm resulted in transverse rms size $\sigma_{xy} = (\sigma_x \sigma_y)^{1/2}$ of 0.38, 0.45, 0.50, 0.61 mm correspondingly. Measured normalized projected emittance is shown in Fig. 2 as a function of the rms laser spot size σ_{xy} . The RF gun launch phase was tuned to yield the maximum mean momentum gain (MMM) of the electron beam except for the BSA=1.5 mm ($\sigma_{xy}=0.38$ mm – the very left data point in Fig. 2) where the gun phase of +6 deg w.r.t. the MMM phase was applied. This deviation is caused by the space charge forces during charge extraction for small laser spot sizes and the high mirror charge at the photo cathode. Increasing of the launch phase of the gun corresponds to higher electric fields at the cathode during charge extraction enabling the production of 2 nC bunch charge at such small laser spot sizes. With operating the gun at MMM phase it was not possible to produce 2 nC at this laser spot size.

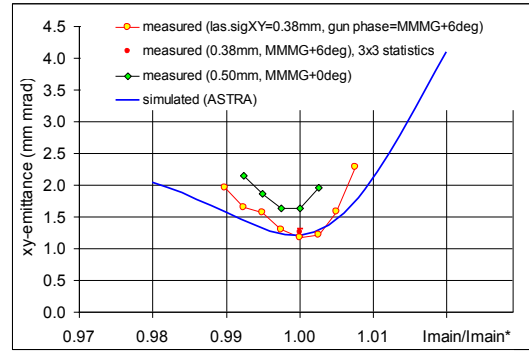


Figure 3: Measured normalized projected emittance as a function of the solenoid current normalized to the optimum value I_{main}/I_{main}^* for 2 nC bunch charge. The optimum main solenoid current I_{main}^* has experimentally been found to be 395 A for both measured curves.

For each laser spot size the solenoid current has been optimized (only the best emittance values are plotted in Fig. 2). The dependence of the measured emittance on the main solenoid tuning is shown in Fig.3 for 2 laser spot sizes $\sigma_{xy}=0.38$ mm and $\sigma_{xy}=0.50$ mm for the gun launch phase of +6 deg and 0 deg w.r.t. to the MMM phase respectively.

The results for the beam dynamics optimization using the ASTRA code [12] is shown in Fig. 3 as well. It should be noticed that the simulated optimum machine setup deviates from the experimentally obtained one. Simulations yield an optimum rms laser spot size of

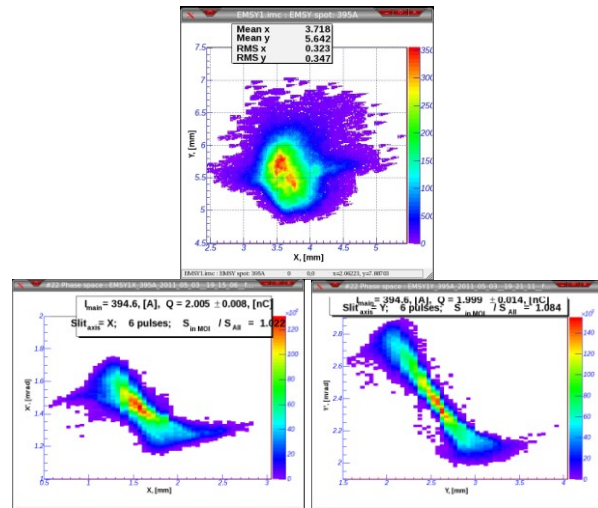


Figure 4: Measured beam distribution (top) horizontal (bottom left) and vertical (bottom right) phase space distributions for a bunch charge of 2 nC. The measurements were performed at the final beam momentum of 24.8 MeV/c, main solenoid current of 395 A, gun RF phase of +6 deg w.r.t. to MMM phase and the booster phase on-crest at maximum acceleration.

0.628 mm and a gun phase of -3.35 deg whereas the experimental optimization resulted in 0.38 mm for +6 deg

and 0.5 mm for 0 deg. One possible explanation is that no Schottky-like effects (charge extraction enhancement due to the presence of a high electric field at the cathode) were applied in the beam dynamics simulations. Partially the discrepancy can also be explained by imperfections of the laser distributions (Fig. 1) and photocathode inhomogeneities whereas ideal profiles have been used in the simulations.

Nine consecutive emittance measurements for the best experimental setup ($\sigma_{xy}=0.38$ mm, gun phase +6 deg w.r.t. to the MMMG phase) resulted in the horizontal and vertical emittance values of (1.24 ± 0.09) mm mrad and (1.27 ± 0.09) mm mrad, respectively. The corresponding xy-emittance value of (1.25 ± 0.06) mm mrad is plotted in Fig. 3 with a red solid circle. The electron beam transverse distribution at the position of the emittance measurement station as well as the horizontal and vertical phase spaces are shown in Fig. 4. A strong nonlinearity of the phase space is a definite signature of the space charge dominated beam. The x-y asymmetry of the beam very probably originates from machine imperfections, detailed investigations are ongoing.

Measured Emittance vs. Bunch Charge

Beam emittance after the photo injector has been optimized at PITZ for a wide range of bunch charges [10] – from 20 pC up to 2 nC. The summary of the emittance measurement at PITZ is shown in Fig. 5.

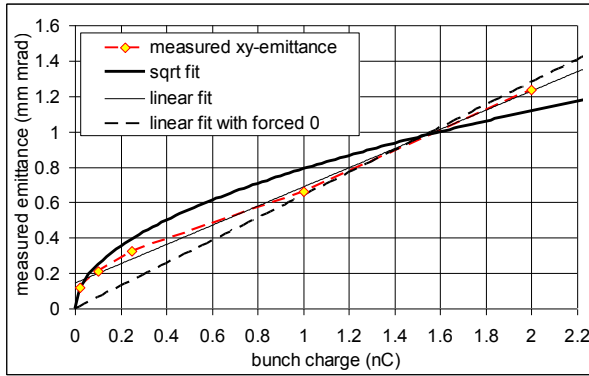


Figure 5: Measured normalized projected emittance as a function of the bunch charge. Square root and two linear fits (with and without offset at zero charge) are plotted as well.

The projected emittance (the geometrical average of horizontal and vertical values) has been optimized for each bunch charge: 0.02; 0.1; 0.25; 1.0 and 2.0 nC. This implies partial optimization of the laser transverse spot size and the gun phase, the main solenoid current has been tuned for each set of these machine parameters. The laser temporal profile has been fixed to be a flat-top with ~ 21 ps FWHM and ~ 2 ps rise and fall time. More details on the emittance optimization for various bunch charges can be found in [10].

The emittance dependence on bunch charge has been fitted with a square root curve and two linear fits: with an

offset at zero charge (solid thin line) and forcing the zero point (dashed black line). One sees that the square root fit is underestimating at charges higher than 1.5 nC whereas both linear fits overestimate the high charge beam emittance.

OPERATION OF FEL WITH HIGH CHARGES

In order to explore the high charge option let us perform a brief analysis for the case of the European XFEL keeping the baseline value of the peak beam current of 5 kA fixed and scaling the emittance linearly and as a square root of charge q . Operation of SASE FELs in a short (around 0.1 nm) wavelength range is well described with the case of optimized XFEL [13]. In this parameter range the peak power in the saturation regime scales inversely proportional to the emittance. As a result, the radiation pulse energy grows proportionally to $q^{1/2}$. For instance, for SASE1 operating at 0.1 nm, we expect an increase of the radiation pulse energy by approximately factor of 2 for the 1 nC case with respect to the 0.25 nC case.

The situation changes qualitatively for the case of SASE3 operating at longer wavelengths. Let us consider the case of SASE3 operating at the energy of 17.5 GeV and radiation wavelength 1.6 nm. The undulator period is equal to 6.8 cm, and the undulator length is equal to 100 m. We fix the peak current to 5 kA, change the bunch charge in the range 0.25 nC – 3 nC and assume emittance scaling as $\varepsilon \propto q^{1/2}$ and $\varepsilon \propto q$ as suggested by the measurements. The reference point is a charge of 1 nC and a normalized emittance of 1 mm mrad. The value of the external beta function is equal to 15 m. This range of FEL parameters corresponds to the diffraction limited (thin) electron beam when saturation length and FEL efficiency at saturation slowly evolve with the value of the emittance, in fact - logarithmically [14]. As a result, we can expect linear growth of the radiation pulse energy with charge. The results of simulations with the code FAST [15] confirm this simple physical consideration (see Fig. 6). Increase of the bunch charge from 0.25 nC to 3 nC results in an increase of the radiation pulse energy nearly by an order of magnitude.

An essential feature of the SASE3 undulator is its extended length for operation as an afterburner of the electron beam used in the SASE1 undulator. This extra undulator length can be effectively used for the undulator tapering and increases the FEL efficiency when operating with "fresh" electron bunches (not disturbed in SASE1). We see from the lower plot in Fig. 6 that pulse energies above 0.2 J can be achieved for $\varepsilon \propto q^{1/2}$. In any case, even for the unfavourable case of $\varepsilon \propto q$, we still can expect significant benefit for SASE3 operation with pulse energies about a factor of 2 above the baseline values for a bunch charge of 1 nC.

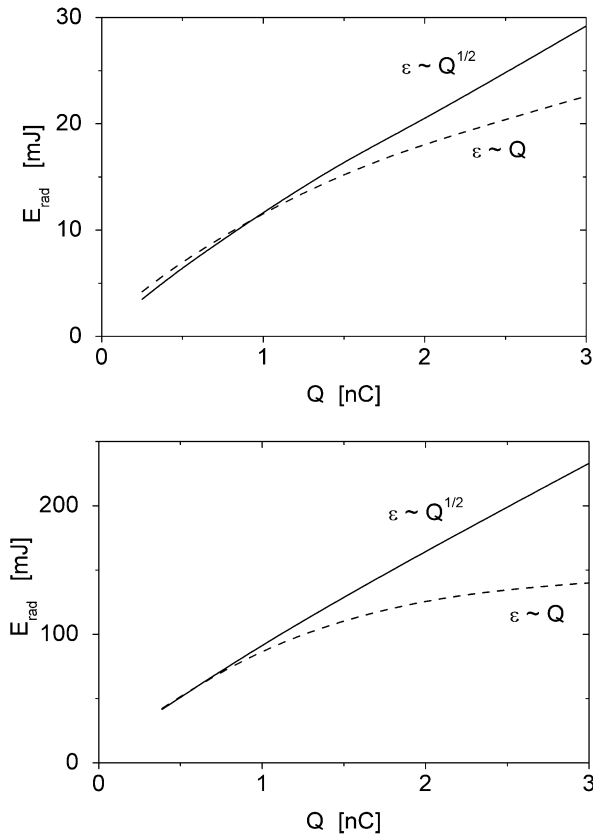


Figure 6: Energy in the radiation pulse versus bunch charge for SASE3 at the European XFEL. Upper plot: FEL operates in the saturation regime. Lower plot: operation with tapered parameters for the undulator length of 100 meters. Electron energy is 17.5 GeV, radiation wavelength is 1.6 nm. Solid and dashed lines correspond to the emittance scaling as $\epsilon \propto q^{1/2}$, and $\epsilon \propto q$, respectively.

The experimental results presented in this paper show that the working space of the charges for the European XFEL can be extended well beyond 1 nC. Within the accuracy of measurements performed at the bunch charge of 2 nC we observe that the scaling of the emittance produced by an optimized XFEL gun lies somewhere in-between of linear and square root dependence on charge. A value of 1.4 mm mrad for the normalized emittance at the charge of 2 nC has been used in the simulations. This implies a certain safety margin to the measured values. SASE FEL simulations based on these assumptions for the electron beam demonstrate the possibility to generate very high pulse energies of $\sim 0.1 \dots 0.2$ J and peak powers above 1 TW in the SASE3 undulator.

CONCLUSIONS

The high charge option for the European XFEL operation has been discussed assuming various dependencies of the beam emittance on the bunch charge. The beam emittance in the photo injector has been experimentally optimized at PITZ for a bunch charge up to 2 nC resulting in an intermediate between linear and square root dependence of the normalized projected

emittance on charge. Based on these dependencies SASE FEL simulations have demonstrated a significant growth of the radiation pulse energy with increased bunch charge.

REFERENCES

- [1] M. Altarelli et al. (Eds.), XFEL: The European X-Ray Free-Electron Laser, Technical Design Report. Preprint DESY 2006-097, DESY, Hamburg, 2006 (see also <http://xfel.desy.de>).
- [2] W. Ackermann et al., Nature Photonics, 1, p. 336, 2007.
- [3] P. Emma et al., Nature Photonics, 4, p. 641, 2010.
- [4] S. Rimjaem et al., Proc. IPAC'10 Conference, Kyoto, Japan, 2010, TUPE011. <http://accelconf.web.cern.ch/AccelConf/IPAC10/papers/tupe011.pdf>.
- [5] I. Zagorodnov and M. Dohlus, Phys. Rev. ST Accel. Beams 14, p. 014403, 2011.
- [6] T. Limberg and W. Decking, Baseline parameters for the electron beam by December 20, 2010.
- [7] T. Tschentscher, Layout of X-Ray Systems, European XFEL Technical Note XFEL.EU TN-2011-001.
- [8] E.A. Schneidmiller, M.V. Yurkov, DESY Print TESLA-FEL 2011-01, Hamburg, 2011.
- [9] M. Dohlus et al., Nucl. Instrum. and Methods A 530 (2004) 217.
- [10] S. Rimjaem et al., "Emittance for different bunch charges at the upgraded PITZ facility", these proceedings, THPA06.
- [11] I. Will and G. Klemz, Optics Express, Vol. 16, No. 9 (2008) 14923-14937.
- [12] K. Flottmann, A Space charge Tracking Algorithm, <http://www.desy.de/~mpyflo/>.
- [13] E.L. Saldin, E.A. Schneidmiller, and M.V. Yurkov, Opt. Commun. 281(2008)1179; New J. Phys. 12 (2010) 035010.
- [14] E.L. Saldin, E.A. Schneidmiller, and M.V. Yurkov, The Physics of Free Electron Lasers (Springer - Verlag, Berlin, 1999).
- [15] E.L. Saldin, E.A. Schneidmiller, and M.V. Yurkov, Nucl. Instrum. and Methods A 429 (1999) 233.